Study of the matter density distributions of halo nuclei ^{6}He and ^{16}C using the binary cluster model

S Q Abdullah[1*] and A N Abdullah[1*]

Department of Physics, College of Science, University of Baghdad, Baghdad, Iraq

Abstract: The harmonic oscillator (HO) and Gaussian (GS) wave functions within the binary cluster model (BCM) have been employ to investigate the ground state neutron, proton and matter densities as well as the elastic form factors of two- neutron ^{6}He and ^{16}C halo nuclei. The long tail is a property that is clearly revealed in the density of the neutrons since it is found in halo orbits. The existence of a long tail in the neutron density distributions of ^{6}He and ^{16}C indicating that these nuclei have a neutron halo structure. Moreover, the matter rms radii and the reaction cross section (σ_R) of these nuclei have been calculated using the Glauber model.

Keywords: Exotic nuclei, neutron halo, Glauber model

1. Introduction

The phenomena of nuclei far from the β-stability it possible to study due to the experimental progress of radioactive ion beams. The neutron halo in some neutron-rich nuclei is one exciting discovery observed by interaction cross section measurements [1,2]. A series of nuclei near the neutron drip line have been identified, in which neutron halo or neutron skin exist [3-5]. However, the behavior of the proton halo is different from the case of the neutron halo because the repulsive Coulomb barrier will be responsible for halo information. The measurements of the reaction cross section (σ_R) have been used to estimate the sizes and matter distributions of exotic nuclei using the optical limit approximation (OLA) of the Glauber model [6].

Alkhazov *et al*. [7] used the Glauber–Sitenko theory to measure the cross sections of ^{6}He, ^{8}He, ^{11}Li, and ^{14}Be using phenomenological nuclear-density distributions with two free parameters. They deduced the nuclear density distribution and rms radii for the nuclei under investigation. Abdullah [8] have investigated the ground state features such as the proton, neutron and matter densities, the root mean square (rms) nuclear radii of unstable neutron-rich ^{6}He, ^{11}Li, ^{14}Be and ^{17}B nuclei using the Bear–Hodgson potential radial wave functions within the three-body model of (Core+2n). The calculated results show the Bear–Hodgson radial

wave functions within the two-body model succeeds in reproducing neutron halo in these nuclei. Abu-Ibrahim *et al*. [9] used the Glauber theory to calculate the σ_R of carbon isotopes with N = 6–16 for wide range of incident energies on a proton target. They are proposed empirical formulas which are useful in predicting unknown cross sections.

In this work, the harmonic oscillator (HO) and Gaussian (GS) wave functions within the binary cluster model (BCM) will be employed to investigate the ground state neutron, proton and matter densities as well as the elastic form factors of two- neutron ^{6}He and ^{16}C halo nuclei. Moreover, the matter rms radii and σ_R of these nuclei will be calculated using the OLA of Glauber model at high energy.

2. Theory

The halo nuclei in BCM [10] are treated as composite projectiles with an A_p mass as core and halo (valence) clusters, in Fig. 1, with masses of A_c and A_v. It is considered that $A_c \geq A_v$. The composite projectile's matter density is given by [11]:

$$\rho_m(r) = \rho_c(r) + \rho_v(r), \quad (1)$$

where the core and valence densities are denoted by $\rho_c(r)$ and $\rho_v(r)$, respectively.

We adopt two distributions in this study, namely; harmonic oscillator (HO) and Gaussian (GS) distributions.

The densities of the core and halo clusters in the HO distribution are described using HO wave functions [12]:

$$\rho_c(r) = \frac{1}{4\pi}\sum_{n\ell} X_c^{n\ell} \left|R_{n\ell}(r, \hat{b}_c)\right|^2 \quad (2)$$

$$\rho_v(r) = \frac{1}{4\pi} X_v^{n\ell} \left|R_{n\ell}(r, \hat{b}_v)\right|^2 \quad (3)$$

In the GS distribution, the GS wave functions are applied to characterize the densities of the core and halo clusters.

Whereas the densities of the core and halo clusters in the GS distribution are described using GS wave functions [10]:

$$\rho_m(r) = A_c\, g^{(3)}(\hat{\alpha}_c, r) + A_v\, g^{(3)}(\hat{\alpha}_v, r), \quad (4)$$

where $g^{(3)}$ is the Gaussian function.

$$g^{(3)}\left(\hat{\alpha}_{c(v)}, r\right) = \frac{1}{\pi^{3/2}\hat{\alpha}_{c(v)}^{3}}\, e^{-r^2/\hat{\alpha}_{c(v)}^{2}}, \qquad \int g^{(3)}\left(\alpha_{c(v)}, r\right) d\vec{r} = 1 \qquad (5)$$

The GS $\left(\hat{\alpha}_c{}^2,\ \hat{\alpha}_v{}^2\right)$ and HO $\left(\hat{b}_c{}^2,\ \hat{b}_v{}^2\right)$ size parameters are given by [10,12]:

$$\hat{g}_c{}^2 = g_c{}^2 + \left(\frac{A_v g}{A_v + A_c}\right)^2, \qquad \hat{g}_v{}^2 = g_v{}^2 + \left(\frac{A_c g}{A_v + A_c}\right)^2, \quad g \equiv \alpha\,, b \qquad (6)$$

The matter density distribution in Eq. (1) can be written in terms of neutron density $[\rho^n(r)]$ and proton density $[\rho^p(r)]$ as follows [13]:

$$\rho_m(r) = \rho^n(r) + \rho^p(r), \qquad (7)$$

where

$$\rho^n(r) = \rho_c^n(r) + \rho_v^n(r) \qquad (8)$$

and

$$\rho^p(r) = \rho_c^p(r) + \rho_v^p(r) \qquad (9)$$

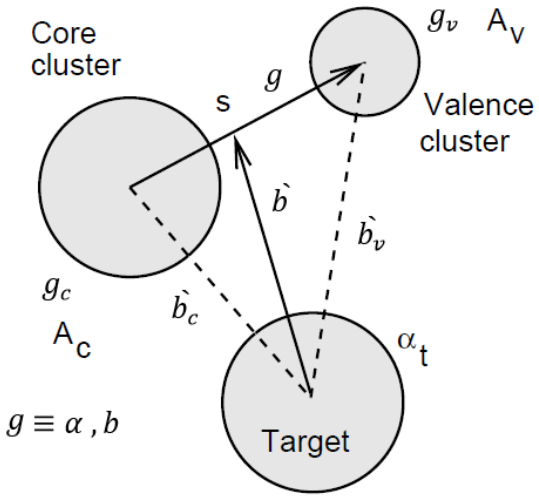

Fig. 1 The target's and two cluster projectile's coordinates [10].

The elastic form factors for investigated nuclei are calculated using the proton densities obtained via HO distributions with the plane wave Born approximation (PWBA), which can be represented as [14]:

$$F(q) = \frac{4\pi}{Z}\int_0^\infty \rho_p(r) j_0(qr) r^2 dr \qquad (10)$$

The GS wave functions within the OLA of the Glauber model has been employ to calculate the σ_R of considered nuclei which can be written as [15]:

$$\sigma_R = 2\pi \int [1 - T(b)]\, b\, db \qquad (11)$$

The $T(b)$ in the OLA is given by [10]:

$$T(b) = \left|S_{el}^{OL}(b)\right|^2 \qquad (12)$$

Where $S_{el}^{OL}(b)$ is given as [10]:

$$S_{el}^{OL}(b) = exp[iO_{PT}(b)] \qquad (13)$$

The overlap $[O_{PT}(b)]$ of the projectile and target ground state densities ($\rho_P$and ρ_T, respectively) is given as [10]:

$$O_{PT}(b) = \int_{-\infty}^{\infty} dR_3 \int d\vec{r}_1 \int d\vec{r}_2 \rho_P(r_1)\rho_T(r_2) f_{NN}\left(\left|\vec{R} + \vec{r}_1 - \vec{r}_2\right|\right) \qquad (14)$$

3. Results and discussion

The BCM with the HO and GS wave functions have been used to study the neutron, proton and matter densities of the ground state as well as the elastic proton form factors of two- neutron ^{6}He (S_{2n}=0.975 MeV, $\tau_{1/2}$= 806 *ms*) and ^{16}C (S_{2n}= 5.46 MeV $\tau_{1/2}$ = 747 *ms*) [16, 17] halo nuclei. We adopt two distributions in BCM calculations namely; HO and GS distributions. Moreover, the matter rms radii and σ_R of these nuclei have been calculated using the OLA of Glauber model.

The HO wave functions are used to describe the densities of the core and halo clusters in the HO distribution. We consider that ^{6}He [^{16}C] is composed of two valence neutrons in $1p_{1/2}$ [$2s_{1/2}$] with ^{4}He [^{14}C] core nucleus which has configuration $(1s_{1/2})^4$ [$(1s_{1/2})^4$, $(1p_{3/2})^8$, $(1p_{1/2})^2$]. The GS wave functions are used to describe the densities of the core and halo clusters in the GS distribution.

The HO and GS size parameters used in present calculations for selected halo nuclei are obtained by Eq. (6) and tabulated in Table 1.

Table 1: The HO and GS size parameters used in present calculations.

Halo Nucleus	Core nucleus	HO		GS	
		$\hat{b}_c$ (fm)	$\hat{b}_v$ (fm)	$\hat{\alpha}_c$ (fm)	$\hat{\alpha}_v$ (fm)
^{6}He	^{4}He	1.413	1.998	1.576	2.450
^{16}C	^{14}C	1.561	2.747	1.759	3.377

The calculated and experimental matter density distributions for ^{6}He (top part) and ^{16}C (bottom part) halo nuclei are depicted in Fig. 2 which are plotted by dotted-dash red curves and gray area [18, 19], respectively. The density distributions of the core and valence two-neutron are also plotted in this figure as the black and green curves. The left and right panels correspond to the densities obtained by GS+GS and HO+HO distributions, respectively. The significant property of the dotted-dash red curves is the long tail (the distinctive property of halo nucleus). We can find that from the above comparison between the calculated and experimental results that the experimental matter density distributions for selected halo nuclei are reproduced well by the present calculations using the GS and HO distributions.

In Fig. 3 the black, green and dotted-dash red curves represented the density of protons, neutrons and matter, respectively. The left and right panels correspond to the densities obtained by GS+GS and HO+HO distributions, respectively. The long tail is a property that is clearly revealed in the density of the neutrons since it is found in halo orbits. Since protons are absent in the halo orbit and all protons of these nuclei are present in their cores, the black curves have a steep slope. The existence of a long tail in the neutron density distributions of ^{6}He and ^{16}C indicating that these nuclei have a neutron halo structure.

In Fig. 4 the dotted-dash red and green curves represented the matter densities of unstable (^{6}He, ^{16}C) and stable (^{4}He, ^{13}C) nuclei, respectively. The dotted-dash red curves extend much farther than the green curves due to the weak binding of the last two-neutron in ^{6}He and ^{16}C.

The proton densities obtained by HO distributions within the PWBA are employ to calculate the elastic form factors of the unstable (^{6}He, ^{16}C) and stable (^{4}He, ^{13}C) nuclei and presented in Fig. 5. In this figure the red and green curves correspond to the calculated C0 form factors of unstable and stable nuclei, respectively whereas the filled circle symbols represented the experimental data of the stable nuclei ^{4}He [20] and ^{13}C [21]. According to these calculated results, that the red and green curves in figure 5 (a) have no diffraction minimum throughout all range of momentum transfer whereas those in figure 5 (b) each has one diffraction minimum. The minimum location of the red curve shifts to the right due to the difference in the center of mass correction.

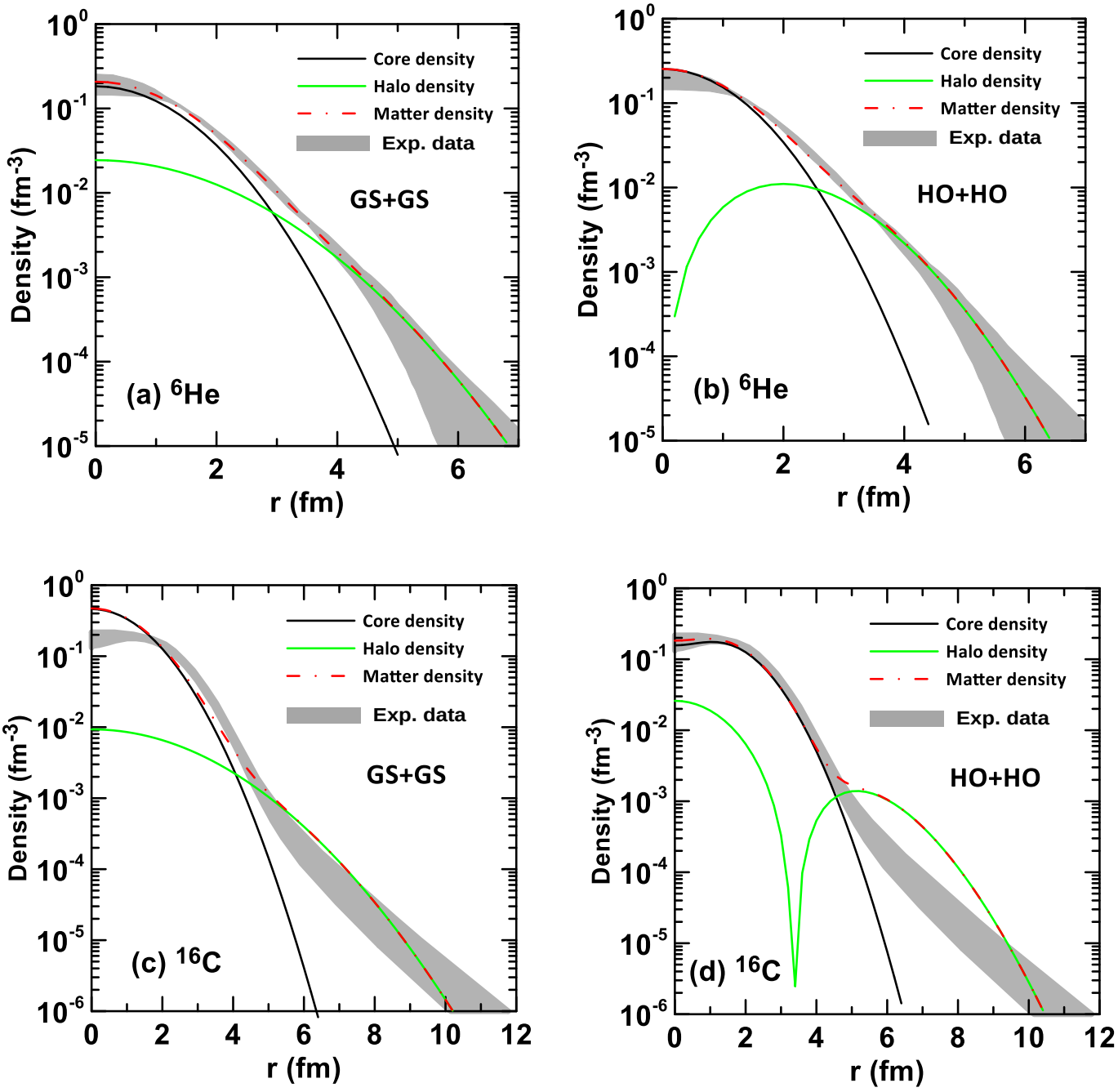

Fig. 2: Calculated and experimental matter densities for ^{6}He and ^{16}C halo nuclei.

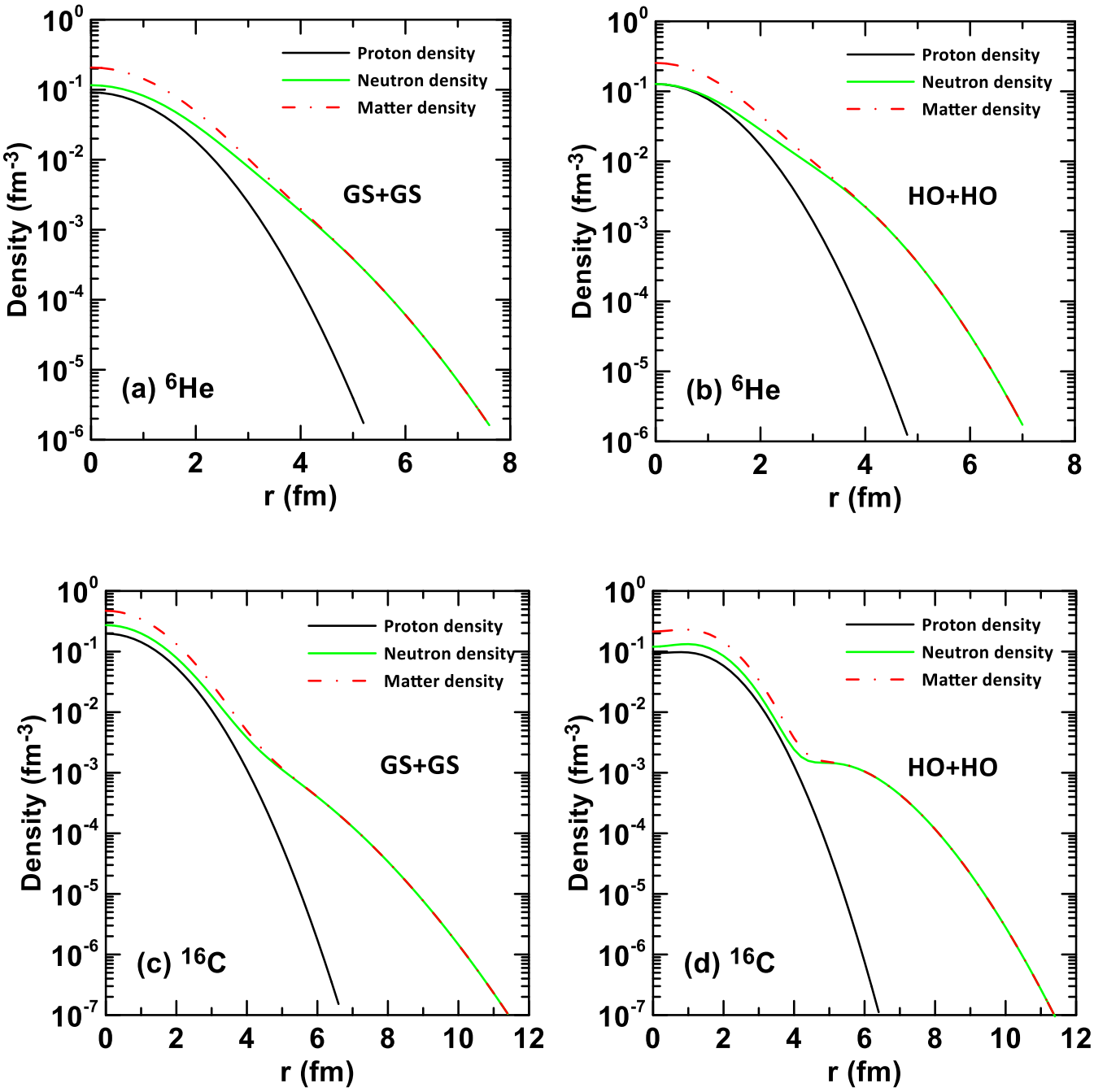

Fig. 3: The matter, proton and neutron densities for ^{6}He and ^{16}C halo nuclei.

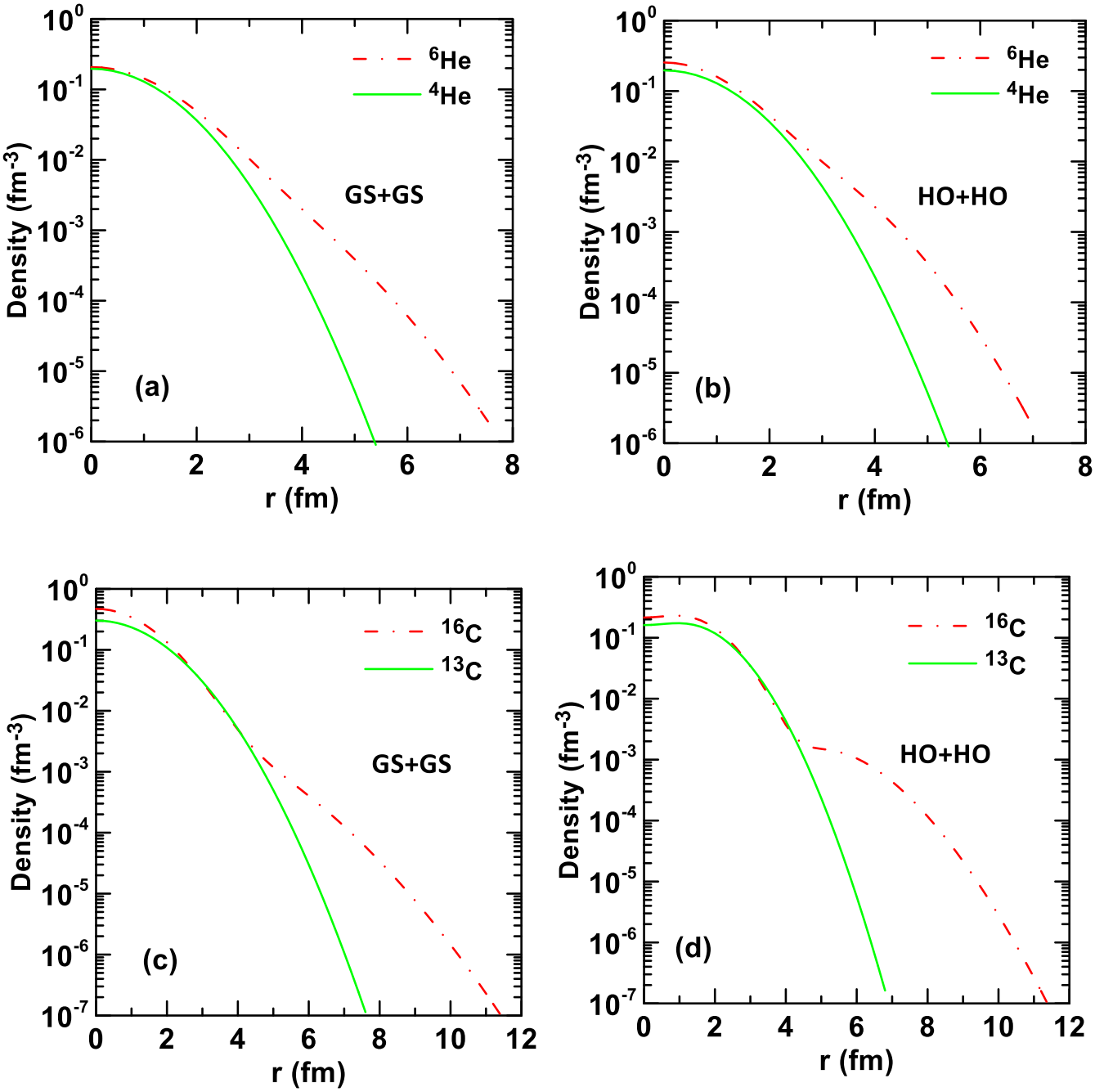

Fig. 4: The calculated matter densities of unstable (^{6}He, ^{16}C) and stable (^{4}He, ^{13}C) nuclei.

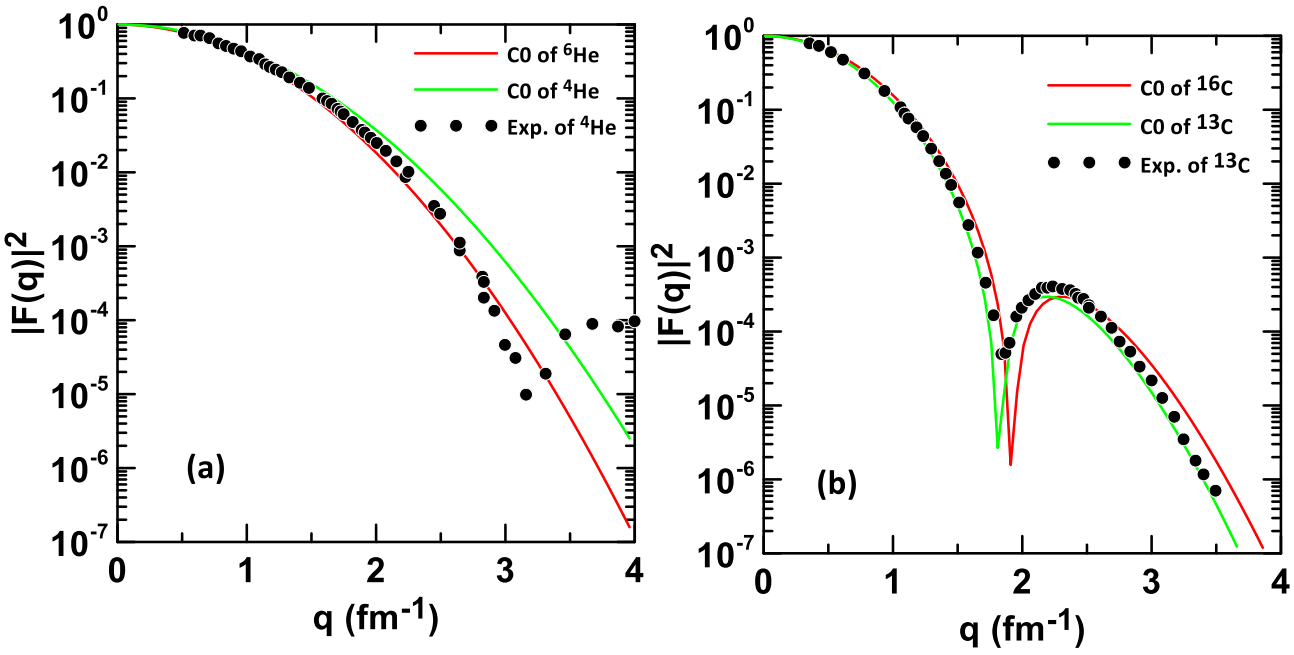

Fig. 5: Elastic form factors of unstable (^{6}He, ^{16}C) and stable (^{4}He, ^{13}C) nuclei.

The GS wave functions within the OLA of the Glauber model has been employed to calculated the σ_R of ^{6}He and ^{16}C nuclei on ^{9}Be target and summarized the obtained results in Table 2 along with the corresponding experimental data [19, 22]. From this table, a good description of experimental σ_R is obtained by the calculated results within quoted error.

Table 2: The experimental and calculated results of σ_R for ^{6}He and ^{16}C halo nuclei.

Halo nuclei	Energy (MeV) [19, 22]	Calculated σ_R (mb)	Experimental σ_R (mb) [19, 22]
^{6}He	790	674	672 ± 7
^{16}C	53	1387	1379 ± 45
	110	1024	1007 ± 42

Figure-5 demonstrates the dependence of the σ_R (in mb), calculated via the OLA of Glauber model, on matter rms radii (in fm) for ^{6}He figure 5 (a) and ^{16}C figure 5 (b) exotic nuclei on

^{12}C target at high energy. The green and horizontal magenta lines are the calculated and experimental σ_R, consecutively, whereas the shaded area refer to the error bar of experimental σ_R. The experimental σ_R for ^{6}He [^{16}C] equal to 722 ± 7 [1036 ± 11] mb at energy 790 [960] MeV. The intersection point of the green line and magenta line refer to the calculated matter rms radius ($\langle r_m^2 \rangle^{1/2}$) of the halo nuclei. We show from figure 5 (a) [figure 5 (b)] that the calculated $\langle r_m^2 \rangle^{1/2}$ of ^{6}He [^{16}C] is equal to 2.53 [2.57] fm which give a good description of experimental data 2.54±0.04 [2.63±0.06] fm [19, 23].

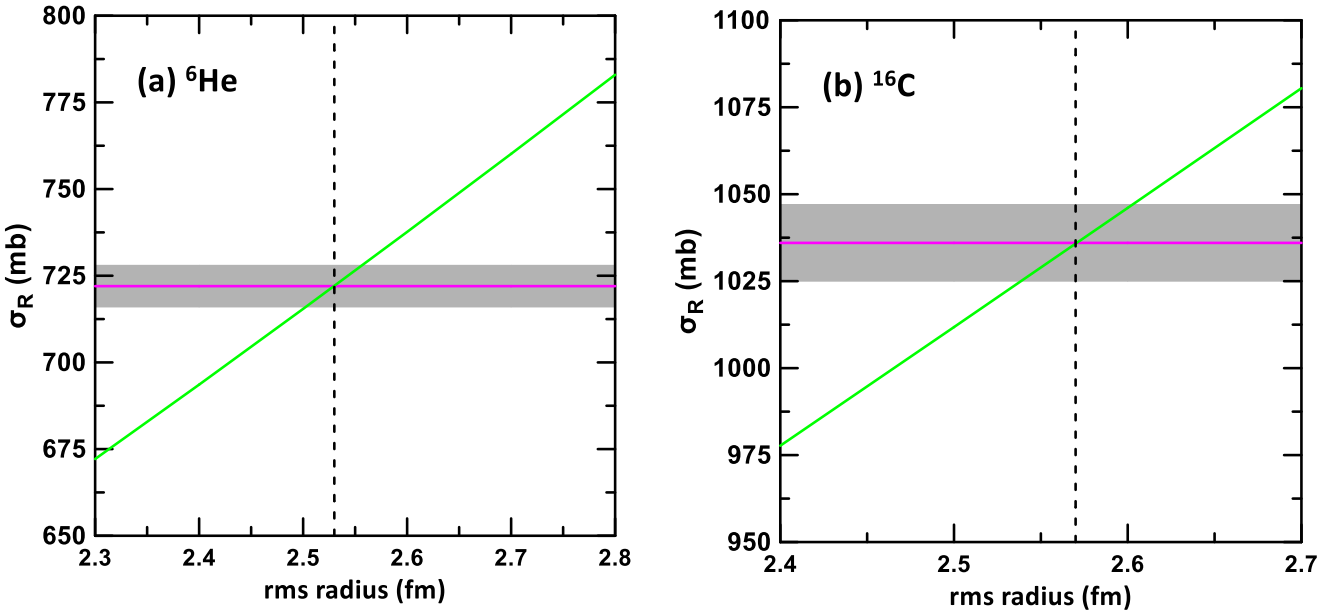

Fig.6: The dependence of the σ_R on the matter rms radii for ^{6}He and ^{16}C halo nuclei.

4. Conclusion

The HO and GS wave functions within the BCM have been employ to investigate the ground state neutron, proton and matter densities as well as the elastic proton form factors of two- neutron ^{6}He and ^{16}C halo nuclei. We adopt two distributions in BCM calculations namely; HO and GS distributions. The experimental matter density distributions for selected halo nuclei are reproduced well by the present calculations using the GS and HO distributions. The long tail is a property that is clearly revealed in the density of the neutrons since it is found in halo orbits. The existence of a long tail in the neutron density distributions of ^{6}He and ^{16}C indicating that these nuclei have a neutron halo structure. Moreover, the matter rms radii and σ_R of these nuclei have been calculated using the OLA of Glauber model. the calculated results of matter rms radii and σ_R give a good description of experimental data.

5. References

[1] I. Tanihata *et al*., *Phys. Rev. Lett.* **55** (1985) 2676.

[2] I. Tanihata *et al*., *Phys. Lett. B* 160 (1985) 380.

[3] I. Tanihata, H. Savajols and R. Kanungo, *Prog. Part. Nucl. Phys.* **68** (2013) 215.

[4] G. A. Korolev *et al.*, *Phys. Lett. B* **780** (2018) 200.

[5] A. V. Dobrovolsky *et al.*, *Nucl. Phys. A* **989** (2019) 40.

[6] A.V. Dobrovolsky *et al.*, *Nucl. Phys.* A **766** (2006) 1.

[7] G. D. Alkhazov *et al.*, *Physics of Atomic Nuclei* **78** (2015) 381.

[8] A. N. Abdullah, *Modern Physics Letters* A **35** (2020) 2050212.

[9] B. Abu-Ibrahim *et al.*, *Phys. Rev*. C **77** (2008) 034607.

[10] J. A. Tostevin, R. C. Johnson, J. S. Al-Khalili, Nucl. Phys. A, 630 (1998) 340c.

[11] A. N. Abdullah, *Pramana – J. Phys.* **94** (2020)154.

[12] A. K. Hamoudi, A. N. Abdullah, Iraqi Journal of Science 57 (2016) 2664.

[13] A. N. Abdullah, *Int. J. Mod. Phys. E* **26** (2017) 1750048.

[14] A.N. Antonov *et al.*, *Int. J. Mod. Phys. E* **13** (2004) 759.

[15] F. D. Qing *et al.*, *Chin. Phys. Lett*. **22** (2005) 572.

[16] M. Wang *et al*., *Chin.* Phys. C 41, 030003 (2017).

[17] G. Audi *et al.*, *Chin.* Phys. C 41, 030001 (2017).

[18] I. Tanihata, H. Savajols and R. Kanungo, *Prog. Part. Nucl. Phys.* **68** (2013) 215.

[19] H. Du *et al.*, ACTA Physica Polonica B **48** (2017) 473.

[20], J. S. McCarthy, I. Sick and R. R. Whitney, *Phys. Rev.* C **15** (**1977**) 1396.

[21] L. A. Schaller *et al.*, Nuclear Physics A 379 (1982) 523.

[22] A. Ozawa, T. Suzuki and I. Tanihata, *Nucl. Phys*. A **693** (2001) 32.

[23] A. N. Antonov *et al.*, *Phys. Rev. C* **72** (2005) 044307.